

Yeast transcriptional device libraries enable precise synthesis of value-added chemicals from methanol

Qiaoyun Zhu¹, Qi Liu¹, Chaoying Yao¹, Yuanxing Zhang^{1,2} and Menghao Cai^{1,3,*}

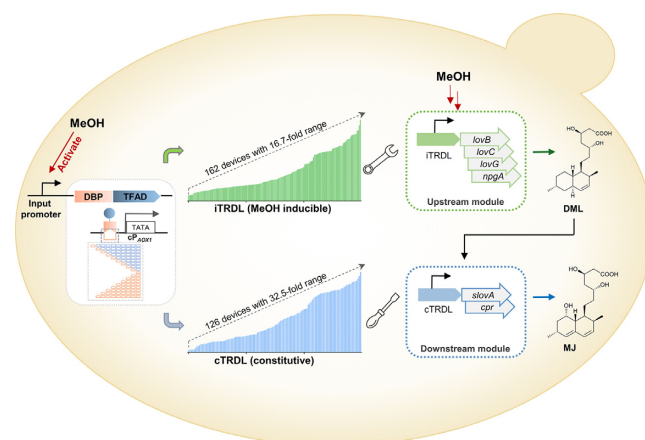
¹State Key Laboratory of Bioreactor Engineering, East China University of Science and Technology, 130 Meilong Road, Shanghai 200237, China, ²Shanghai Collaborative Innovation Center for Biomanufacturing, 130 Meilong Road, Shanghai 200237, China and ³Shanghai Frontiers Science Center of Optogenetic Techniques for Cell Metabolism, East China University of Science and Technology, 130 Meilong Road, Shanghai 200237, China

Received May 09, 2022; Revised August 08, 2022; Editorial Decision August 09, 2022; Accepted August 25, 2022

ABSTRACT

Natural methylotrophs are attractive methanol utilization hosts, but lack flexible expression tools. In this study, we developed yeast transcriptional device libraries for precise synthesis of value-added chemicals from methanol. We synthesized transcriptional devices by fusing bacterial DNA-binding proteins (DBPs) with yeast transactivation domains, and linking bacterial binding sequences (BSs) with the yeast core promoter. Three DBP–BS pairs showed good activity when working with transactivation domains and the core promoter of P_{AOX1} in the methylotrophic yeast, *Pichia pastoris*. Fine-tuning of the tandem BSs, spacers and differentiated input promoters further enabled a constitutive transcriptional device library (cTRDL) composed of 126 transcriptional devices with an expression strength of 16–520% and an inducible TRDL (iTRDL) composed of 162 methanol-inducible transcriptional devices with an expression strength of 30–500%, compared with P_{AOX1} . Selected devices from iTRDL were adapted to the dihydromonacolin L biosynthetic pathway by orthogonal experimental design, reaching 5.5-fold the production from the P_{AOX1} -driven pathway. The full factorial design of the selected devices from the cTRDL was adapted to the downstream pathway of dihydromonacolin L to monacolin J. Monacolin J production from methanol reached 3.0-fold the production from the P_{AOX1} -driven pathway. Our engineered toolsets ensured multilevel pathway control of chemical synthesis in methylotrophic yeasts.

GRAPHICAL ABSTRACT



INTRODUCTION

In view of its quantitative, predictive and engineering characteristics, synthetic biology has pushed forward the conversion of life cognition to life design. Recently, the development of theories and methods in synthetic and molecular biology has allowed the sophisticated rewiring of non-natural life. Most successes have been achieved on model microbial hosts, such as *Escherichia coli* (1,2) and *Saccharomyces cerevisiae* (3,4), whereas other non-conventional hosts have not been explored. As different strains have different genetic backgrounds, they may have specific biological components that adapt to different application scenarios. Therefore, exploration of individualized set-ups for different strains is required.

For instance, the bio-utilization of sustainable one-carbon (C1) substrates such as methanol, methane and CO₂ has attracted widespread attention in both academia and industry (5). Methanol is a major byproduct of the fossil industry and a promising product of methane oxidation or CO₂ reduction. It represents a probable C1 substrate for industrial bio-utilization, with its liquid state being compatible for transportation and fermentation con-

*To whom correspondence should be addressed. Tel: +86 21 64253286; Fax: +86 21 64253286; Email: cmh022199@ecust.edu.cn

trol (6–8). Moreover, methanol has a 50% higher degree of reduction per mole of carbon than sugar substrates such as glucose, and thus provides more surplus electrons for compound synthesis (9). With mature genetic manipulation tools, some non-methylotrophic strains, such as *E. coli* (10–12), *Corynebacterium glutamicum* (13–15) and *S. cerevisiae* (16–18), have been engineered to utilize methanol by the re-assembly of exogenous methanol assimilation pathways in cells. Nevertheless, their weak methanol utilization ability still lags far behind their production requirements (19). Instead, natural methylotrophs are known to efficiently utilize methanol, but lack sufficient genetic tools to enable multi-gene pathways (20–22).

In the past two decades, the methylotrophic yeast, *Pichia pastoris* (syn. *Komagataella phaffii*), has been shown to be an excellent workhorse for protein production (20,23–25) and a potential cell factory for chemical synthesis (26–29). This organism can efficiently utilize methanol with high-level expression of endogenous alcohol oxidase 1 (Aox1) and thus grows well on methanol as the sole carbon source (22). Most recently, it was further developed as an autotrophic strain capable of growth on CO₂ with methanol as a reducing power donor (30,31). The extraordinary characteristics of high cell density, strong expression ability and availability of post-translational modifications (20) support expression of enzymes which catalyse the synthesis of the desired products. Recently, Golden Gate, CRISPR–Cas9 and other genome editing strategies have facilitated pathway assembly in *P. pastoris* (32–40). Nevertheless, high-level biosynthesis of these products requires precise control of the multigene pathway, including an increase in precursor pools, up-regulation of positive pathways, down-regulation of competitive pathways and balance of pathway parts (28,29,41). In comparison with model expression hosts, *P. pastoris* lacks fine-tuned expression tools (21). Although promoters can be bioinformatically screened, it is difficult to obtain promoters with a broad range of expression levels and clear transcriptional regulatory mechanisms that can adapt to complicated pathway expression. Promoter engineering may provide variants of gradient strengths from either methanol-inducible (42,43) or other types (44–48) of promoters. However, these variants are obtained mainly through simple mutations or combinations of DNA sequences. They may share most DNA sequences or *in situ* transcription factors (TFs), which can easily cause uncontrollable cross-talk during transcription (49–51). Therefore, it is necessary to propose alternative expression toolboxes for non-conventional yeasts.

In recent years, synthetic TFs with heterologous DNA-binding and transactivation domains have been designed to function with regulatory *cis*-elements. These engineered devices have demonstrated functional independence over native transcriptional regulation in various microbial species (52,53). Previously, we explored a transcriptional signal amplification device (TSAD) in *P. pastoris* composed of a hybrid promoter *lacO*-cP_{AOXI} (core P_{AOXI}) and a chimeric transactivator LacI–Mit1AD (29). An improved TSAD (iT-SAD) was obtained using 18 combination groups of *cis*- and *trans*-acting elements in *E. coli* and *P. pastoris*. The reporter protein expressed by the iTSAD with glucose was 4.2-fold higher than that expressed by the strong methanol-

inducible promoter P_{AOXI} with methanol (54). This represents a useful strategy that far exceeds the amplification of the P_{AOXI} variant library (up to 1.6-fold) (42,43).

The functions of iTSAD inspired us to explore the synthetic transcriptional components of the full coverage intensity. This could be realized by combinatorial assembly of various *cis*- and *trans*-acting elements from bacteria and yeast, and by manipulation of the spacers between the binding and core sequences of the *cis*-acting elements. Constitutive control of these elements enabled a synthetic constitutive transcriptional device library (cTRDL) composed of 126 devices with an intensity range of 16–520% (P_{AOXI} as 100%). Methanol-inducible input promoters with gradient strength were used to construct a synthetic methanol-inducible TRDL (iTRDL) composed of 162 devices with an intensity range of 30–500% (P_{AOXI} as 100%). We subsequently tested the applicability of the iTRDL and cTRDL in multigene pathway expression and balance. We selected devices from the iTRDL to adapt to dihydromonacolin L (DML) biosynthesis from methanol using an orthogonal experimental design, which led to a 5.5-fold DML titre compared with that from the P_{AOXI}-driven pathway. Furthermore, the selected devices from the cTRDL were adapted to the downstream pathway of DML to monacolin J (MJ) using a full factorial design. It finally achieved a 3.0-fold MJ titre compared with that from the P_{AOXI}-driven pathway with methanol as the substrate. Our study provides an alternative expression toolbox and a strategy for methanol bio-utilization in natural methylotrophs.

MATERIALS AND METHODS

Strains and growth conditions

The plasmids and strains used in this study are listed in Supplementary Table S5 and S6, respectively. *Pichia pastoris* strains GS115, GS_P_{AOXI}-G and GS_cP_{AOXI}-G, and the yeast expression vectors pPIC3.5 K, pPIC Z B and pGAPZ B were stored in our laboratory. *Escherichia coli* Top10 was purchased from Invitrogen. The plasmids BB1_12, BB1_23, BB1_34, BB2_AB, BB2_BC and BB3eN_14 for GoldenPiCS cloning were purchased from Addgene (#98549). The plasmids pP-P_{AOXI}G (pP-GFP), pPcAG, pPlacOncAG ($n = 1–9$), pParaIcAG, pGP_{GAP}LacIP1AD, pGP_{GAP}LacIX1AD, pGP_{GAP}LacIM1AD, pGP_{GAP}AraCM1AD, pZ_BCGN and pK_sAR were constructed and stored in our laboratory (28,29,32,43,54). *Escherichia coli* was incubated at 37°C in LLB medium (0.5% yeast extract, 1% tryptone and 0.5% NaCl). Antibiotics (100 µg/ml ampicillin or 50 µg/ml zeocin) were added when required. *Pichia pastoris* was incubated at 30°C in YPD (1% yeast extract, 2% tryptone and 2% glucose) or MGY (0.67% YNB and 1% glycerol) medium for cell growth. To screen *P. pastoris* transformants, YPD or MGY medium was supplemented with the appropriate antibiotics (100 µg/ml zeocin, 750 µg/ml hygromycin B and 100 µg/ml nourseothricin) or histidine (20 µg/ml). *Pichia pastoris* was cultured in YNM medium (1.34% YNB and 0.5% methanol) for reporter protein expression or in YNMB medium (YNM with 0.3% K₂HPO₄ and 1.18% KH₂PO₄) for compound production. A solid medium was obtained by adding 2% agar.

Plasmid and strain construction

Oligonucleotides were synthesized by Suzhou Genewiz Biotech Co., Ltd, China and are listed in Supplementary Table S7. The plasmids used in this study were constructed by seamless cloning and/or Gibson assembly (ClonExpress™ II one-step cloning kit, VazymeBiotech Co., Ltd, China). Molecular genetic analyses of *E. coli* and *P. pastoris* were performed as previously described (29,54). The construction details of the plasmids and strains are described in supplementary Materials and methods.

Fluorescence and transcriptional analysis

The strain stored at -80°C (20 μl) was transferred into 2 ml of fresh YPD medium in a 20 ml serum bottle and cultivated for 2 days for strain activation. Yeast broth was inoculated into fresh YPD medium for pre-culturing to an optical density (OD_{600}) of 6.0. The cells were harvested by centrifugation (5000 \times g, 5 min), washed twice with sterile water and then distributed to the required medium (YNM) to a final OD_{600} of 1.0 for culture in a 24-well plate (<4 ml of liquid in each 10 ml well). The cell broth was collected at 12, 18 and 24 h and washed twice with sterile water for fluorescence determination. Reporter enhanced green fluorescent protein (eGFP) fluorescence (normalized to OD_{600}) of the cultured samples was analysed using a multimode microplate reader (Synergy 2, BioTek Instruments, USA) at an excitation wavelength of 485 nm and an emission wavelength of 525 nm (gain, 60 nm). Transcriptional levels of biosynthetic genes were tested to evaluate their relationships with MJ and DML production among the different strains. The details of transcriptional analysis were described in supplementary Materials and methods.

Cell growth analysis

The growth of strains carrying synthetic TFs (sTFs) and eGFP expression cassettes driven by various promoters was analysed in a shake-flask culture. *Pichia pastoris* GS115 was used as the control strain (wild-type, WT). Cells were pre-cultivated overnight in 50 ml of YPD medium after activation from storage (-80°C). Then, 200 μl of culture broth was transferred into 50 ml of YPD medium in a 250 ml shake flask and grown to OD_{600} . Cells were harvested by centrifugation (5000 \times g, 5 min), washed twice with sterile water and resuspended in YNB medium. Finally, the cells were inoculated into YNM medium at a final OD_{600} of 1.0 for growth measurement. Samples were collected and measured every 4 h. Three biological replicates were used for each strain.

Production and detection of MJ and intermediates

Cells resuspended in YNB medium were then inoculated into YNMB medium to produce the desired compounds at a suitable cell density. During culture, methanol was added separately to an appropriate level every 24 h. Culture broth was collected at certain time intervals, extracted using a suitable volume of ethyl acetate and vortexed for 3 min. The organic phase was evaporated under reduced

pressure and dissolved in methanol. The extracts were analysed by high-performance liquid chromatography (HPLC) equipped with a C18 column (Kromasil™, Sweden; 250 mm \times 4.6 mm \times 5 mm, 100 Å spherical silica) using a gradient elution strategy at 1 ml/min. The mobile phase consisted of HPLC-grade H_2O containing 0.1% acetic acid (A) and HPLC-grade acetonitrile (B).

Statistical analysis

Data were obtained from three biological replicates assayed in at least two experimental batches and are presented as the mean \pm standard deviation. Data were analysed using GraphPad Prism (version 7.04). The unpaired two-tailed Student's *t*-test was used to assess differences among the grouped data. Statistical significance was set at $P < 0.05$.

RESULTS

Engineering of the cTRDL with constitutively varied expression strength

The transcription of protein-coding genes in eukaryotes begins with the assembly of RNA polymerase II and general TFs on promoter DNA (55). A transcriptional activator harbouring a separate N-terminal DNA-binding domain and C-terminal activation domain is essential for this process (55). For example, the most typical yeast transactivator, Gal4, binds to regulatory sites on the *GALI* promoter naturally. The activation domain of Gal4 fused to the bacterial regulator LexA (DNA-binding protein) was then expressed in yeast together with a reporter plasmid bearing LexA-binding sites upstream of the *GALI* promoter. The chimeric protein successfully activated reporter transcription (55). This method further allows different applications of domain-swapped and function-extended biological TFs (53,56). We previously identified a Zn(II)2Cys6-type transactivator, Mit1, with a separable DNA-binding domain interacting with P_{AOX1} (a strong and widely used methanol-inducible promoter) and an activation domain that helps recruit RNA polymerase II in *P. pastoris* (57). Using the domain-swapping strategy, we constructed TSAD using an sTF of LacI–Mit1AD (*E. coli lac* regulator fused with the activation domain of Mit1) and a hybrid promoter of *lacO*– cP_{AOX1} (*E. coli lac* operator linked to the core region of P_{AOX1}) (29). The improvement of the functional components further generated an iTSAD with high expression capacity (54). These preliminary results provide the basic structure of the transcriptional device libraries that we aimed to develop in this study.

A synthetic transcriptional device mainly carries four components: a DNA-binding protein (DBP), binding sequence (BS), TF activation domain (TFAD) and core promoter (CP). Therefore, the combination of diverse DBP–BS and TFAD–CP may lead to the development of various engineered devices (Figure 1A). We first selected different bacterial regulators, LacI (29), AraC (54), LexA (58), AcrR and BetI (59), as DBPs to fuse with Mit1AD using a GGGGS linker (Supplementary Figure S1; Supplementary Table S1). An SV40 nuclear localization sequence (NLS) was fused at the N-terminus of DBPs (except LacI) to allow them to enter the nucleus of *P. pastoris*. LacI was able

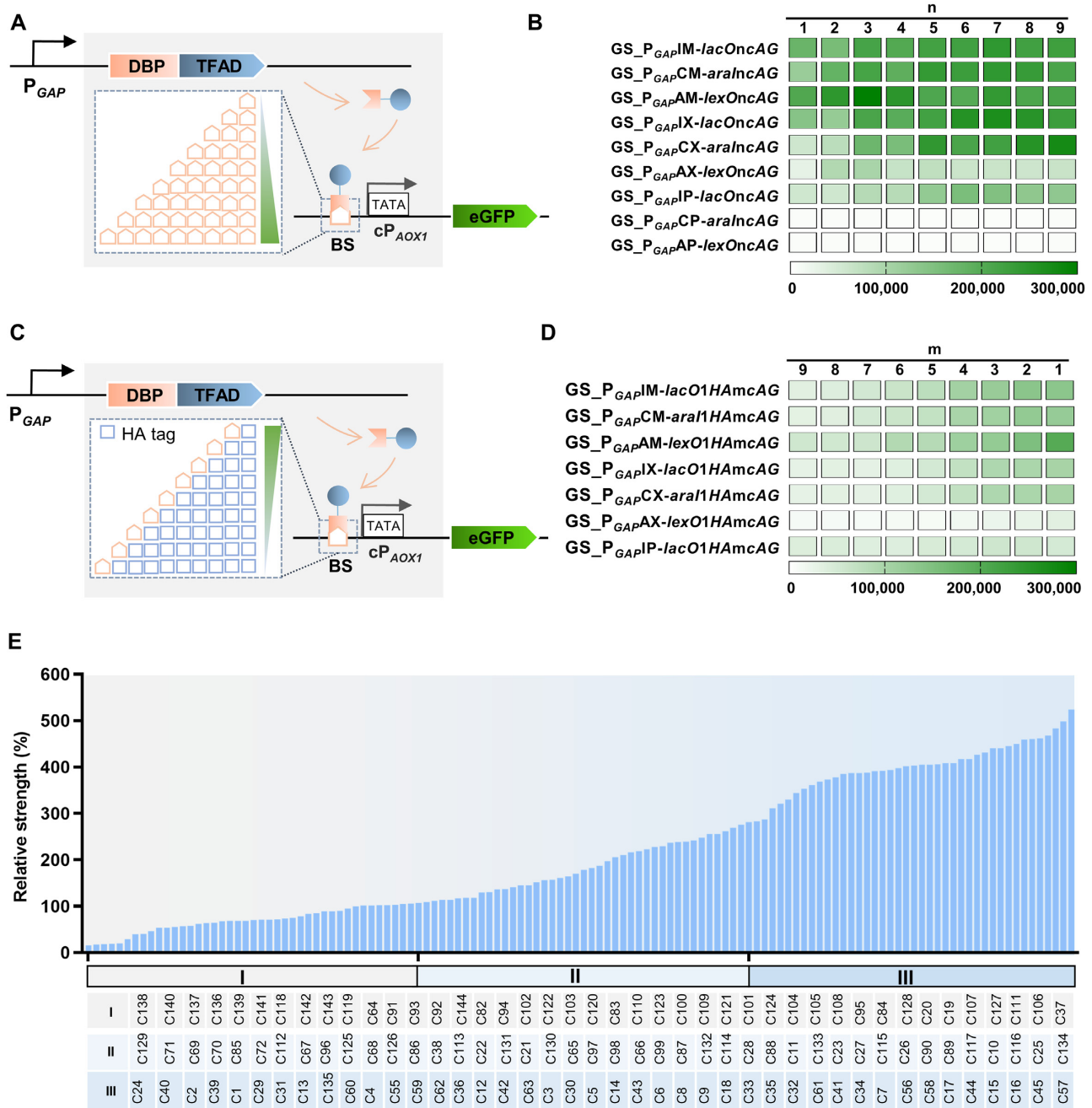


Figure 1. Design and characterization of the cTRDL. (A) Genetic circuit scheme of the cTRDL with increased regulator BSs. A chimeric transactivator composed of a DBP and a TFAD is driven by an input promoter. It targets the BSs located upstream of *cP_{AOX1}* and recruits RNA polymerase to activate transcription of the gene of interest. (B) Heatmaps showing the fluorescence intensity of the diverse devices. Three DBPs fused with three TFADs (Supplementary Figure S1) to generate nine chimeric transactivators, i.e. LacI–MitIAD (IM), AraC–MitIAD (CM), LexA–MitIAD (AM), LacI–MxrIAD (IX), AraC–MxrIAD (CX), LexA–MxrIAD (AX), LacI–PrmIAD (IP), AraC–PrmIAD (CP) and LexA–PrmIAD (AP). Tandem copies ($n = 1–9$) of BSs (*lacO*, *araI* and *lexO*) were linked with *cP_{AOX1}* to obtain synthetic promoters. *cA* represents *cP_{AOX1}* and *G* indicates eGFP. The eGFPs expressed by the cTRDL were tested in methanol medium (YNM). The detected fluorescence data for each subset of cTRDLs are shown in Supplementary Figure S2. (C) Genetic circuit scheme of the cTRDL with increased spacers between BSs and *cP_{AOX1}*. Tandem copies ($m = 1–9$) of *HA* spacer were inserted between one BS and *cP_{AOX1}* to fine-tune the output strength of the cTRDL. (D) Heatmaps showing the fluorescence intensity of the diverse devices. Nine chimeric transactivators were described in (B). Each activator was paired with a single copy of a specific BS which was spaced apart from *cP_{AOX1}* by 1–9 copies of *HA* spacers. *cA* and *G* were the same as in (B). The detected fluorescence data for each subset of cTRDLs are shown in Supplementary Figure S3. (E) Full functional devices in the cTRDL with smoothly increasing output strength. A total of 126 devices are included (exclusion of 18 inactive ones) from all the constructs in (B) and (D). Chimeric transactivators were controlled by the constitutive promoter *P_{GAP}*. The serial number (Supplementary Table S2) for each column is marked sequentially below the figure, which corresponds to region I, II and III, respectively, on the horizontal axis.

to localize to the *P. pastoris* nucleus without an NLS (29). These five engineered sTFs, driven by the constitutive promoter P_{GAP} , were tested to determine whether they activate eGFP expression when interacting with their specific operators *lacO*, *araI*, *lexO*, *acrAB* and *bet* linked by cP_{AOXI} (Supplementary Figure S1; Supplementary Table S1). Almost no cross-talk was observed between the different sTFs and the hybrid promoters (Supplementary Figure S1). LacI, AraC and LexA functioned well; therefore, they were selected for fusion with the activation domains of the transactivators Mit1, Mxr1 and Prm1 (57,60,61). Nine cross combinations were constructed to work with the corresponding hybrid promoters. Mit1AD-derived sTFs strongly activated eGFP expression with the tested promoters (Figure 1B; Supplementary Figure S2A, D, G). Mxr1AD-derived sTFs strongly activated eGFP expression with *lacO*- cP_{AOXI} and *araI*- cP_{AOXI} but weakly with *lexO*- cP_{AOXI} (Figure 1B; Supplementary Figure S2B, E, H). In contrast, the Prm1AD-derived sTFs weakly activated eGFP expression with *lacO*- cP_{AOXI} but were inactivated with *araI*- cP_{AOXI} and *lexO*- cP_{AOXI} (Figure 1B; Supplementary Figure S2C, F, I). Their diverse expression levels further led us to employ a tandem BS for adjusting the activation strength. Tandem fragments of 1–9 *lacO*, *araI* and *lexO* were synthesized and fused with cP_{AOXI} (Figure 1A). Generally, tandem BSs remarkably improved eGFP expression, despite the optimal number being BS dependent (Figure 1B). Among them all, LexA–Mit1AD/*lexO3*- cP_{AOXI} presented the strongest expression capacity [5.2-fold of that of P_{AOXI} in methanol medium (YNM), Supplementary Figure S2G], surpassing our previously constructed iTSAD (54) (4.0-fold of P_{AOXI} in YNM tested in this study) (Supplementary Figure S2A).

Hitherto, these constructed devices mostly showed expression levels over the strong promoter P_{AOXI} . For precise pathway expression, a full range of devices with varying intensities is indispensable. Therefore, we designed devices with a decreased intensity. As previously reported, the distance between the upstream activation sequences and TATA box of the promoter affects promoter strength in yeast (62). We inserted various copies of a non-functional haemagglutinin (HA) coding sequence as a spacer between a single BS and the CP (not transcribed at this locus) to regulate the output strength of the devices (Figure 1C). The fluorescence intensity generally decreased with an increase in the tandem number of HA spacers (Figure 1D; Supplementary Figure S3). A series of successively weakened devices were obtained, among which LexA–Mxr1AD/*lexO1HA9*- cP_{AOXI} presented the weakest expression level of only 16% relative to P_{AOXI} (Figure 1D; Supplementary Figure S3G). Taken together, all constructed devices constituted a fine-tuned cTRDL with a broad range of expression levels (Figure 1E; Supplementary Table S2). It includes 126 synthetic devices covering an expression strength of 16–520% (tunable range of 32.5-fold) compared with P_{AOXI} (referred to as 100%). Moreover, the strength of the commonly used constitutive promoter P_{GAP} in *P. pastoris* was approximately one-third that of methanol-inducible P_{AOXI} (51, verified in our lab). Therefore, our engineering cTRDL output reached ~60–1650% of the intensity of P_{GAP} . Overall, we provide a constitutive expression toolbox that far exceeds conventional P_{GAP} promoter variants (44,45).

Engineering of the iTRDL with inducibly varied expression strength

Genes can be expressed in the induction mode using inducible promoters. By inducible expression, the cell growth and production phases are separated to relieve the metabolic burden from recombinant proteins or their catalytic products (63,64). Therefore, we designed an iTRDL for flexible expression control of product synthesis from methanol.

The overexpression of TFs may impair cell growth and metabolism in methanol (65). Thus, we first selected various methanol-inducible promoters, such as P_{AOX2} , P_{FGH1} , P_{PEX5} , P_{TAL2} , P_{FBA2} , P_{FLD1} , P_{CAT1} , P_{DAS1} and P_{AOX1} (51,66), to drive sTFs (specifically LacI–TFADs) and analysed their effects on cell growth. These promoters were first tested in a methanol medium (YNM) to verify their differential expression activities (Supplementary Figure S4). The growth of strains containing LacI–TFADs driven by these promoters was tested correspondingly (Supplementary Figure S5). We found that the growth of strains carrying LacI–Mit1AD was severely impaired by all promoters except for the weakest P_{AOX2} . Impairment of cell growth was also observed in strains harbouring LacI–Mxr1AD with promoters stronger than P_{FLD1} . In contrast, strains harbouring LacI–Prm1AD grew normally, except those driven by the strongest P_{AOX1} . To retain Mit1AD-derived synthetic devices, we used the methanol-inducible promoter P_{0374} (66) to drive LexA–Mit1AD, which did not impair cell growth (Supplementary Figure S5).

Subsequently, various sTFs were expressed by their adaptive inducible promoters to work with hybrid promoters harbouring tandem operators and spacers, as described in the cTRDL (Figure 2A). As anticipated, increased copies of BS improved the output strength, and increased copies of the spacer permitted a decrease in the output strength of devices with various sTFs (Figure 2B; Supplementary Figure S6A–I). Generally, synthetic devices harbouring Mxr1AD or Mit1AD are stronger than those harbouring Prm1AD. We obtained the strongest device LexA–Mit1AD/*lexO3*- cP_{AOXI} with the input promoter P_{0374} (Figure 2B; Supplementary Figure S6C) and the weakest device LacI–Prm1AD/*lacO1HA8*- cP_{AOXI} with the input promoter P_{DAS1} (Figure 2B; Supplementary Figure S6G). Finally, they constituted a fine-tuned iTRDL containing 162 methanol-inducible synthetic devices (Figure 2C; Supplementary Table S2). The iTRDL covers an expression strength of 30–500% (tunable range of 16.7-fold) compared with methanol-inducible P_{AOXI} (referred to as 100%). Therefore, we provided a methanol-responsive expression toolbox that far exceeds that of the P_{AOXI} promoter variants (42,43).

iTRDL devices adapted for upstream pathway improved synthesis of the intermediate product dihydromonacolin L from methanol

Currently, heterologous synthesis of complicated compounds via microbial systems is often inefficient because of low yield and intermediate accumulation. Pathway balancing has been used as a prioritized strategy for solving such problems (41). Our synthetic transcriptional de-

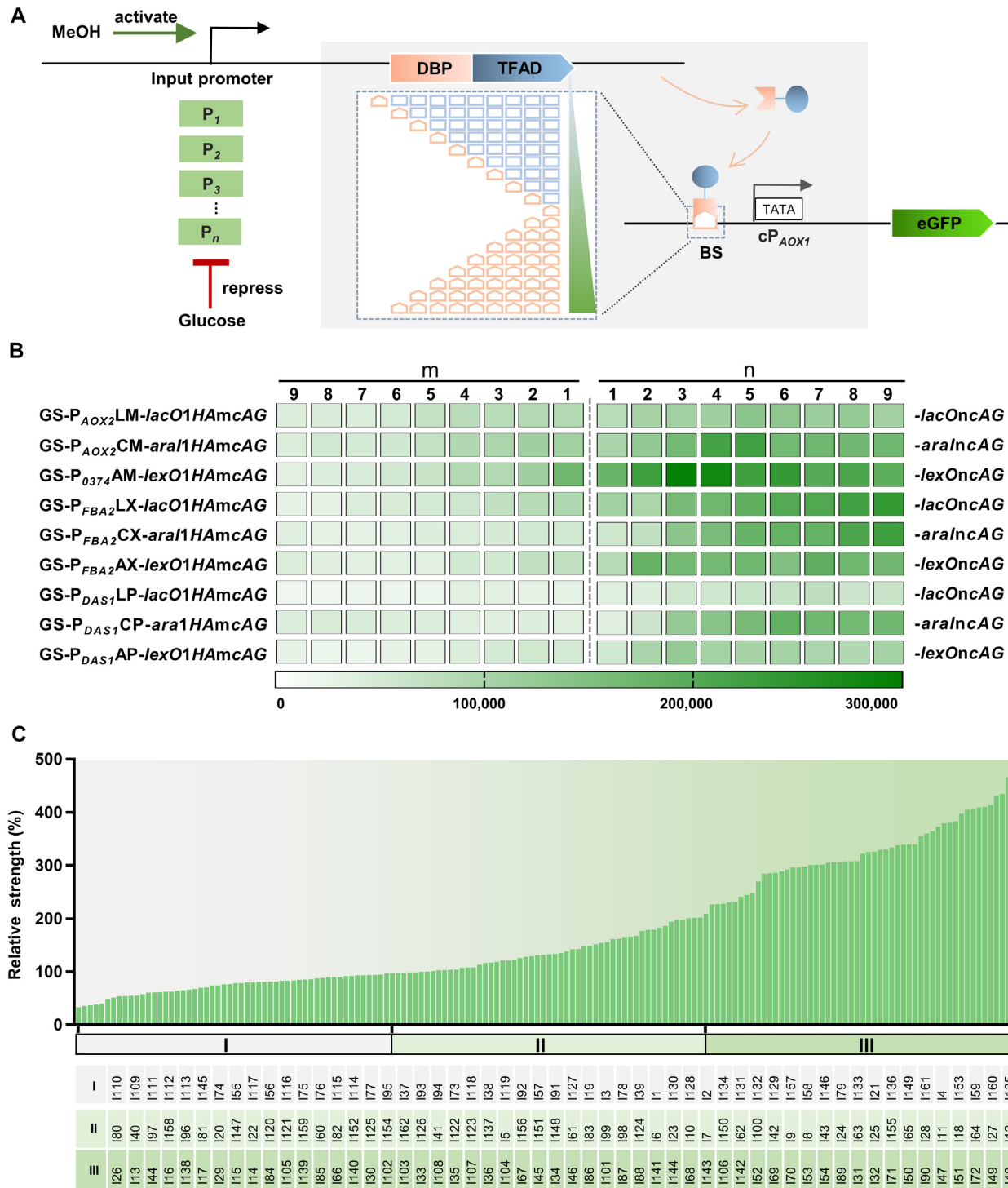


Figure 2. Design and characterization of the methanol-inducible iTRDL. (A) Genetic circuit scheme of iTRDL. Four available methanol-inducible promoters were identified from 10 candidates, which were of different strength (Supplementary Figure S4) and favoured cell growth when expressing specific chimeric transactivators (Supplementary Figure S5). These four promoters, i.e. P_{0374} , P_{AOX2} , P_{DAS1} and P_{FBA2} , were used to drive the diverse chimeric transactivators verified in Figure 1, which can target the BSs of various hybrid promoters. Increased tandem copies of BSs and *HA* spacer were also adopted in this design to adjust device strength. (B) Heatmaps showing the fluorescence intensity of the diverse devices. Three DBPs fused with three TFADs (Supplementary Figure S1) to generate nine chimeric transactivators as described in Figure 1. Different chimeric transactivators were controlled by P_{0374} , P_{AOX2} , P_{DAS1} and P_{FBA2} correspondingly as determined in Supplementary Figure S6. Tandem copies ($n = 1-9$) of BSs (*lacO*, *araI* and *lexO*) were linked with cP_{AOX1} to obtain synthetic promoters. Also, tandem copies ($m = 1-9$) of *HA* spacer were inserted between one BS and cP_{AOX1} to further fine-tune the output strength of the iTRDL. *cA* represents cP_{AOX1} and *G* indicates eGFP. eGFPs expressed by the iTRDL were tested in methanol medium (YNM). The detected fluorescence data for each subset of the iTRDL are shown in Supplementary Figure S6. (C) Full functional devices in the iTRDL with smoothly increasing output strength. A total of 162 devices are included from all the constructs in (B). The serial number (Supplementary Table S2) for each column is marked sequentially below the figure, which corresponds to region I, II and III, respectively, on the horizontal axis.

vices offer new choices for fine-tuning pathway control in methylotrophic yeast. We then tested the applicability of the cTRDL and iTRDL in combinatorial control of biosynthetic pathways. We used MJ, which is a critical substrate for the semi-synthesis of the commercial hypolipidaemic drug simvastatin, as a reporter compound. MJ is synthesized via the fungal polyketide pathway and involves six enzymes: nonaketide synthase (LovB), enoyl reductase (LovC), thioesterase (LovG), phosphopantetheinyl transferase (NpgA), cytochrome P450 (LovA) and cytochrome P450 oxidoreductase (CPR) (28).

We split the full pathway into an upstream polyketone synthesis module and a downstream oxidation module. The methanol-inducible iTRDL was first applied to the upstream module to separate the cell growth and production phases (Figure 3A). This module contains four enzymes, LovB, LovC, NpgA and LovG, which synthesize the intermediate DML. To precisely balance the DML pathway, we used a statistical method, an orthogonal experimental design, involving four factors (enzyme-coding genes) and three expression levels (selected devices from the iTRDL). Two previously constructed strains, *Pp/P_{AOXI}-BCGN* (D1 and D9), were used as control groups, in which biosynthetic genes were recognized as single-copy (D1) or multicopy (D9), driven by *P_{AOXI}* (28,67). We selected devices with expression strengths not lower than that of *P_{AOXI}* for this experimental design. Moreover, methanol-inducible promoters with an expression intensity of >200% (relative to *P_{AOXI}*) have seldom been reported. To test the effectiveness of our devices, we set the three expression levels to ~100, 250 and 450% (Supplementary Table S3) to adapt to the four biosynthetic genes, thus generating nine experimental groups (A1–A9) (Supplementary Table S4; Figure 3B).

We then selected suitable devices from the iTRDL, i.e. *P_{FBA2}LacI-Mxr1AD* paired with *HA2lacO1cP_{AOXI}* (~100%; Device No. I62), *lacO3cP_{AOXI}* (~250%; Device No. I66) and *lacO9cP_{AOXI}* (~450%; Device No. I72) (Supplementary Table S2), to regulate the expression of biosynthetic genes (Figure 3C). Finally, we successfully obtained strains of *Pp/iTRDL-BCGN* (A1–A9) with the desired genotypes, all of which were identified as carrying single-copy gene cassettes. Subsequently, the strains were cultured for DML synthesis in methanol (YNMB medium). Notably, the resulting DML titre varied greatly among the nine experimental groups (Figure 3C), illustrating that the expression levels of biosynthetic enzymes significantly affected pathway balancing. These results also proved that our methanol-inducible iTRDL effectively regulates various pathway nodes. The A3 strain with LovB expression by the strongest device (~450%), but LovC, LovG and NpgA by the weakest device (~100%), produced the highest level of DML (250.0 mg/l). DML production by A3 reached 5.2- and 1.9-fold that by the *P_{AOXI}*-based single-copy control (D1) and multicopy control (D9), respectively (Figure 3C). In addition, the calculated DML productivity (per cell density) of A3 was 8.2- and 3.5-fold that of D1 and D9, respectively. Data analysis of the orthogonal experimental design showed a high range (*R*)-value for LovG and LovB, indicating that these two enzymes highly influenced DML synthesis (Supplementary Table S4). *K*-value analysis predicted an optimal combination of LovB (~450%), LovC

(~250%), LovG (~100%) and NpgA (~250%). Therefore, we constructed this strain (Opt), which further improved the DML titre (by 6.0%) and productivity (by 11.4%) compared with strain A3. The growth of these strains was also determined (Figure 3D). The overexpression of biosynthetic enzymes imposes a metabolic burden on cells, thus affecting cell growth. Compared with strain D1 with single-copy genes expressed by *P_{AOXI}*, the growth of strains with either multicopy genes driven by *P_{AOXI}* (D9) or single-copy genes driven by iTRDL devices (A1–A9, Opt) was relatively weak.

Adaptation of iTRDL and cTRDL devices for downstream pathway improved synthesis of the final product MJ from methanol

DML was oxidized to the final product MJ by the downstream module with LovA and its partner CPR (Figure 4A). We further tested the adaptation of the iTRDL and cTRDL devices to the downstream pathway for MJ synthesis. Independent DBP–BS pairs are necessary to reduce transcriptional cross-talk between the upstream and downstream modules. Thus, we chose LexA–Mit1AD, but not LacI–Mit1AD, as the downstream module (Figure 4B), considering the non-interactive relationship between LacI–*lacO* and LexA–*lexO* (Supplementary Figure S1), and non-interaction between Mit1 and Mxr1 (57).

We hypothesized that the accumulation of downstream enzymes prior to the induction of the upstream module might accelerate the conversion of the intermediate to the final product. Therefore, the devices selected from cTRDL were first used for downstream pathway assembly. The Opt strain producing DML (Figure 3C) was used as the parent strain. Similar to the upstream module, devices with expression levels of ~100, 250 and 450% (referred to as *P_{AOXI}*) were adapted for codon-optimized LovA (sLovA) and CPR. We then selected appropriate constitutive devices from cTRDL, i.e. *P_{GAP}LexA-Mit1AD* paired with *lexO1HA8cP_{AOXI}* (~100%; Device No. C128), *lexO1HA3cP_{AOXI}* (~250%; Device No. C133) and *lexO3cP_{AOXI}* (~500%; Device No. C57) (Supplementary Table S2). A full factorial design of these devices adapted with sLovA and CPR was performed, and nine recombinant strains were generated and designated as *Pp/iTRDL-BCGN_cTRDL-sAR* (OC1–OC9). Similarly, our previously constructed *Pp/P_{AOXI}-BCGN_sAR* strains, J1 (single copy of sLovA and CPR expressed in D9) and J9 (multicopy of sLovA and CPR expressed in D9) (28,67) were used as controls. We grew 11 strains directly in methanol medium (YNMB) with an initial OD₆₀₀ of 1.0, similar to the culture of strains harbouring the upstream module. However, an extremely low MJ titre was observed with the accumulation of intermediates (Supplementary Figure S7A), as well as severe growth impairment (Supplementary Figure S8A). We suspected that the continued expression and accumulation of sLovA and CPR by cTRDL devices resulted in a metabolic burden on the cells. Then, inducible devices from iTRDL with comparative strengths were used, i.e. *P₀₃₇₄LexA-Mit1AD* paired with *lexO1HA8cP_{AOXI}* (~100%; Device No. I38), *lexO1HA3cP_{AOXI}* (~250%; Device No. I43) and *lexO3cP_{AOXI}* (~500%; Device No. I48). A full factorial de-

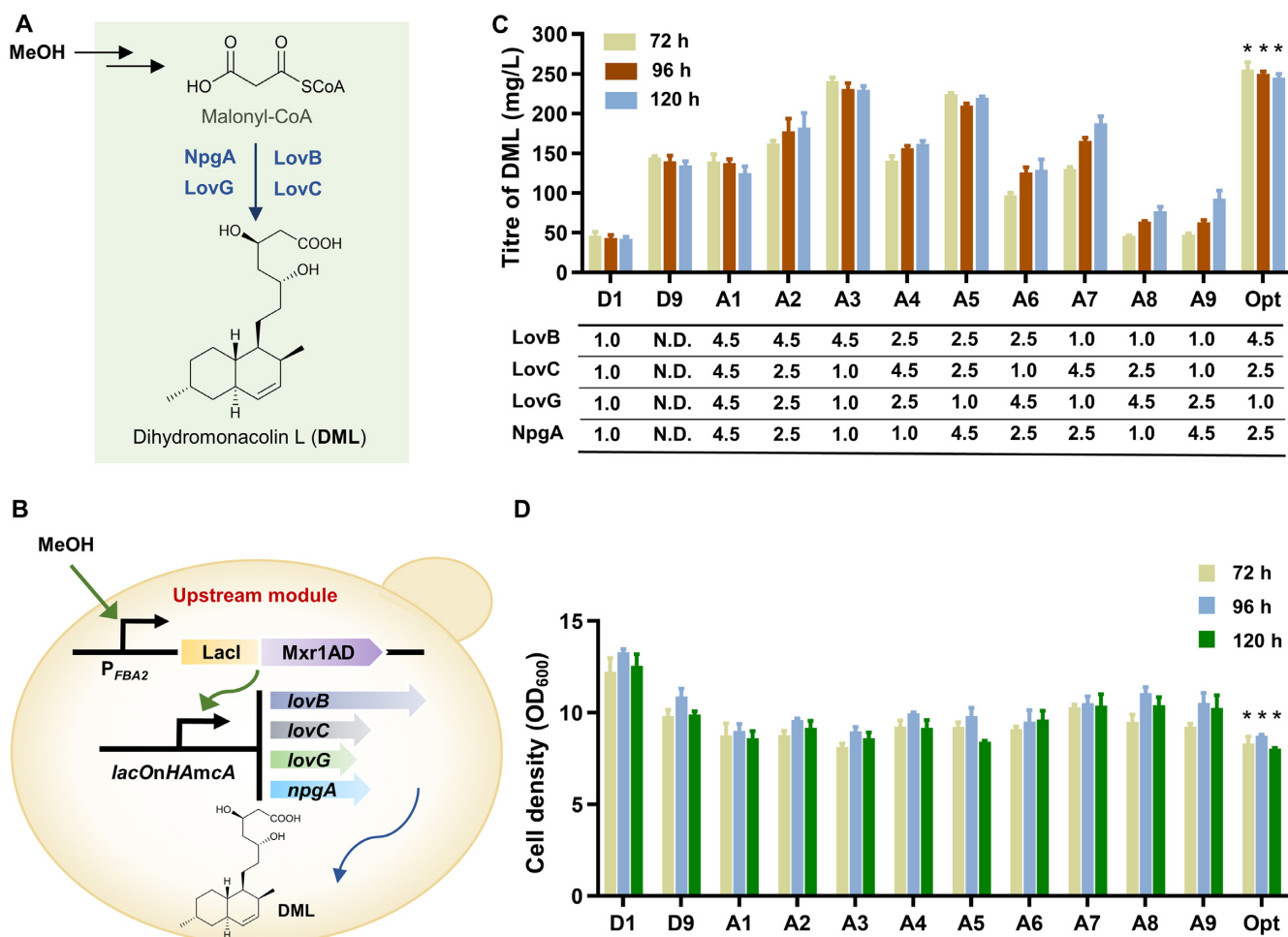


Figure 3. Orthogonal experimental design of iTRDL devices matching upstream pathway nodes for the fine-tuning synthesis of DML from methanol. (A) Biosynthetic pathway of DML used for evaluation of the iTRDL. It involves four enzymes: LovB, LovC, LovG and NpgA (28). We expressed these genes as an upstream module for the full MJ pathway. (B) Design scheme for fine-tuning production of DML by iTRDL devices. The LacI-Mxr1AD-derived devices from iTRDL were used. The corresponding hybrid promoters of *lacOnHAMcA* (various numbers of *lacO* and *HA* linked with *cP_{AOX1}*) were used for differential expression of biosynthetic genes, respectively. (C) DML biosynthesis by separate control of pathway nodes with iTRDL devices. Devices were selected from the library subset described in (B). We employed the orthogonal experimental design method with four factors (genes) and three levels (output strengths of devices) to evaluate the fine-tuning functions of the iTRDL. The three expression levels were set as ~100% (1.0-fold), ~250% (2.5-fold) and ~450% (4.5-fold) relative to *P_{AOX1}* to adapt to the four pathway genes separately (Supplementary Table S3). Thus, devices Nos I62, I66 and I72 in Figure 2C were used. Nine recombinant single-copy strains, *Pp/iTRDL-BCGN* (A1–A9), were obtained with correct genotypes. *K*-value analysis from the experimental data predicted an optimal expression combination of LovB (4.5-fold), LovC (2.5-fold), LovG (1.0-fold) and NpgA (2.5-fold). It then led to a strain with this optimal combination (designated as Opt). In contrast, two previously constructed high-yield strains, i.e. D1 (single-copy strain) and D9 (optimum multicopy strain), were used as control groups, in which each biosynthetic gene was driven by the *P_{AOX1}* (28,67). These strains were grown in glucose medium (YPD) and then shifted to methanol medium (YNMB) to the final density at an OD₆₀₀ of 1.0 for incubation. N.D., not detected. (D) Cell growth of various DML-producing strains from (C). Error bars represent the standard deviation of three biological replicates assayed in duplicate or triplicate. Statistical significance of the DML titre and cell growth of Opt relative to other strains is shown at different time points (**P* < 0.05 at 72, 96 and 120 h, respectively).

sign adapted with sLovA and CPR produced nine recombinant single-copy strains of *Pp/iTRDL-BCGN*. iTRDL-sAR (OI1–OI9). However, similar growth and production problems were also observed (Supplementary Figures S7B and S8B). Therefore, the expression mode of the downstream module is not the cause of this problem.

We further evaluated the culturing processes of these strains. For either cTRDL- or iTRDL-derived strains, full pathway genes will continue to be expressed after their inoculation into the methanol medium (YNMB). Therefore, the resulting metabolic burden began to impair cell growth at very low cell density (OD₆₀₀ = 1.0). However, in practi-

cal fermentation, cell growth and inducible production are typically separated. We then applied this strategy to culture the MJ-producing strains. The strains were grown in glucose medium (YPD) to enrich the cells, which were then transferred into a methanol medium (YNMB) at a higher density (OD₆₀₀ = 10.0) (Figure 4C, D). Although the high expression of pathway enzymes by the cTRDL and iTRDL reduced cell growth during the production phase (Figure 4C, D), MJ synthesis by either the cTRDL or iTRDL was greatly improved by this strategy (Figure 4E, F). Co-expression of sLovA with an intensity of ~250% and CPR with an intensity of ~100% (OI4 and OC4) promoted high-

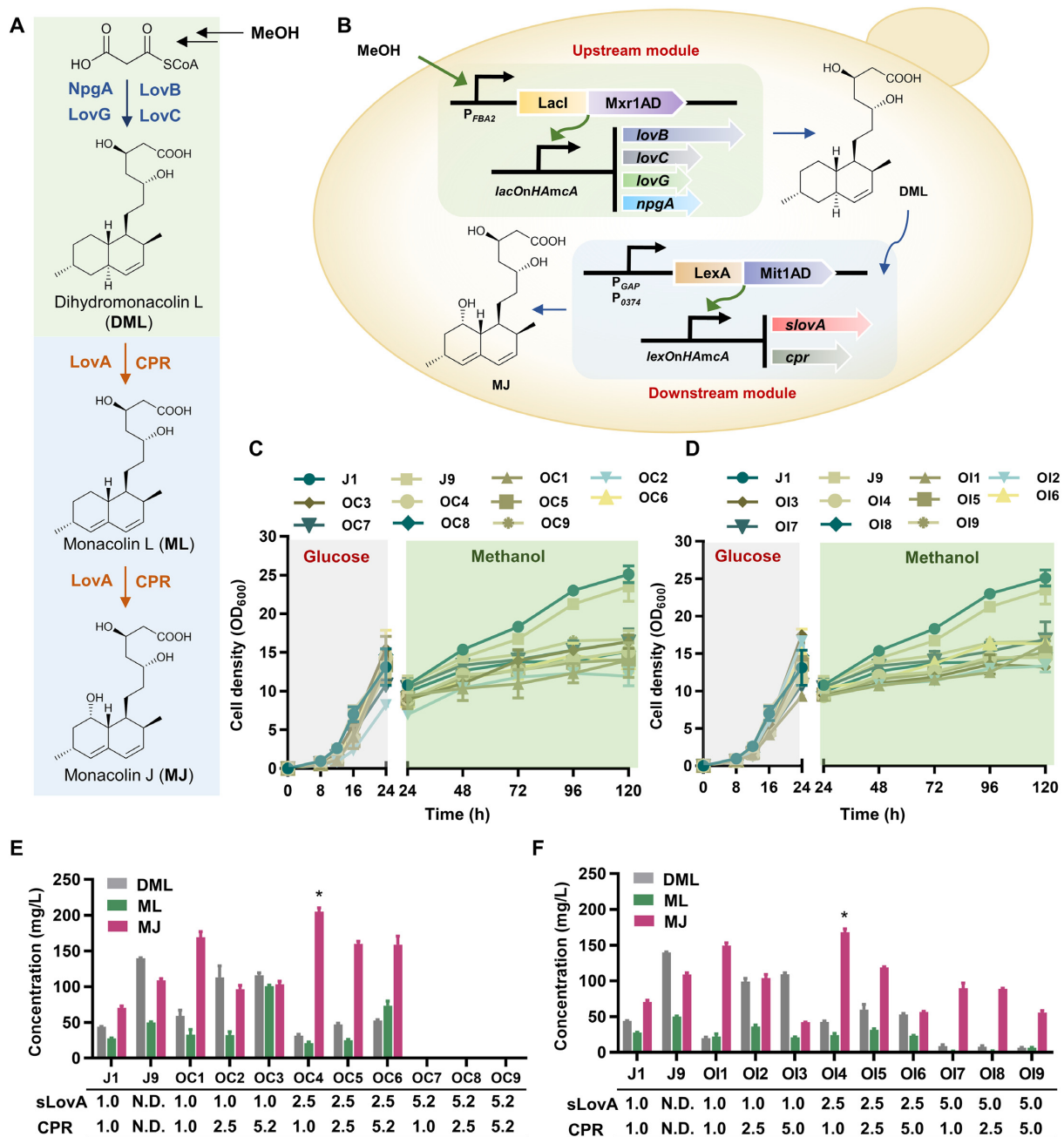


Figure 4. Full factorial design of iTRDL and cTRDL devices matching downstream pathway nodes to adapt to the optimal upstream module for the fine-tuning synthesis of MJ from methanol. (A) The biosynthetic pathway of MJ consisting of the upstream DML module and the downstream DML to MJ module was reasssembled. The upstream module is described in Figure 3. The defined downstream module carries sLovA and CPR that mediate double oxidation steps to transform DML to the final product MJ (28). (B) Design scheme for fine-tuning production of MJ by iTRDL and cTRDL devices. The Opt strain from Figure 3 was used as the parent host. We employed the LexA–Mit1AD-derived devices in the downstream module to avoid the cross-talk with LacI–Mxr1AD in the upstream module. The subset of LexA–Mit1AD-derived devices from cTRDL and from iTRDL were used. The corresponding hybrid promoters of *lexOnHAmcA* (various numbers of *lexO* and the *HA* spacer linked with *cP_{AOX1}*) were used for differential expression of sLovA and CPR, respectively. Time profiles of cell growth of strain Opt equipped with the downstream cTRDL driving module (C) and iTRDL driving module (D). We selected constitutive devices (C128, C133 and C57 in Figure 1E) of three varying strengths [100% (1.0-fold), 250% (2.5-fold) and 520% (5.2-fold) relative to *P_{AOX1}*] and methanol-inducible devices (I38, I43, I48 in Figure 2C) of three varying strengths [100% (1.0-fold), ~250% (2.5-fold) and 500% (5.0-fold) relative to *P_{AOX1}*] from the subset of LexA–Mit1AD-derived devices described in (B). Full factorial constitutive or inducible devices matching downstream pathway nodes were designed. It resulted in two groups of single-copy strains, i.e. *Pp/iTRDL-BCGN_cTRDL-sAR* (OC1–OC9) and *Pp/iTRDL-BCGN_iTRDL-sAR* (OI1–OI9) (E and F). These strains were grown in glucose medium (YPD) and then shifted to methanol medium (YNMB) to the final density at an OD₆₀₀ of 10.0 for incubation. As a control, two previously constructed high-production strains, i.e. J1 (single copy of sLovA and CPR expressed in D9) and J9 (multicopy of sLovA and CPR expressed in D9), were used, in which each biosynthetic gene was driven by the native *P_{AOX1}* separately (28,67). (E and F) The titre of the final product MJ and the intermediates of DML and ML were analysed after 96 h culture of the OC strains (E) and OI strains (F). N.D., not detected. The error bars represent the standard deviation of three biological replicates assayed in duplicate or triplicate. Statistical significance of the MJ titre of OC4 and OI4, relative to other corresponding strains, is shown (**P* < 0.05).

level production of MJ with minor accumulation of intermediates. However, excessive expression of sLovA had negative effects on MJ synthesis, leading to low titres of MJ in the OI7, OI8 and OI9 strains, and almost no titre in the OC7, OC8 and OC9 strains. Finally, the OI4 and OC4 strains produced 172 and 208 mg/l MJs, respectively. The constitutive expression of sLovA and CPR by the cTRDL surpassed their inducible expression by the iTRDL when adapted to the inducible expression mode of the upstream module by the iTRDL. MJ production of strain OC4 by selected devices from the cTRDL reached 3.0-fold that of the single-copy control J1 and 1.8-fold that of the multicopy control J9 by P_{AOXI} . The results illustrate that the strengthening and balancing of the pathway nodes inside and between the two modules can be precisely controlled. We offer new toolboxes for the high-level biosynthesis of heterologous chemicals from methanol in yeast.

DISCUSSION

Although remarkable progress has been made in reprogramming bacteria and baker's yeast into synthetic methylotrophs (10–18), breakthroughs in the methanol utilization capacity for industrial use remain a huge challenge (19,68). The production of chemicals by natural methylotrophs has provided an alternative path to methanol bio-utilization for industrial purposes (28,69–71). However, the lack of genetic tools severely prevents natural methylotrophs from synthesizing valuable chemicals via multigene pathways (20–22). Although the methylotrophic yeast *P. pastoris* has been used as an attractive protein expression host (20,23–25), its use for the production of chemicals via complicated pathways is still limited by insufficient fine-tuning expression tools (21).

In this study, we demonstrated that transcriptional device libraries with broad expression levels and smooth changes can be achieved by rational design in addition to conventional promoter variants. We engineered sTFs by fusing endogenous TFADs with different bacterial DBPs, in which hybrid *cis*-elements were designed by linking DBP-paired BSs and TFAD-contributing CPs. Three workable bacterial DBP–BS pairs with minimal cross-talk, LacI–*lacO*, LexA–*lexO* and AraC–*araI*, were selected from the five tested groups (Supplementary Figure S1). Their combinations with activation domains of three *P. pastoris* TFs, Mit1, Mxr1 and Prm1 (57), finally generated a cTRDL with 126 constitutive transcriptional devices when the TFs were constitutively expressed (Figure 1; Supplementary Figures S2 and S3). Subsequently, methanol-inducible promoters with gradually changing strengths were used to drive sTFs, thus generating an iTRDL with 162 methanol-inducible transcriptional devices (Figure 2; Supplementary Figure S3). With regard to the strength of the native P_{AOXI} (100%), our engineered cTRDL and iTRDL presented expression intensity ranges of 16–520% and 30–500%, respectively. They provide diverse and powerful expression tools compared with traditional promoter variants. In addition, the minimal cross-talk among various sTF–BS pairs may extend their application scenarios, which shows a unique advantage over the reported promoter libraries (42–45,48).

The synthetic cTRDL and iTRDL were then tested to fine-tune the multigene biosynthetic pathway of the hy-

polipidaemic drug intermediate, MJ. The six essential genes of the MJ biosynthetic pathway were divided into two modules. Thus, we evaluated the regulatory functions of the selected cTRDL and iTRDL devices within each module and between the two modules. The statistical method of orthogonal experimental design was employed to arrange three expression levels of devices from the iTRDL, matching the four biosynthetic genes for the upstream module. The resulting nine single-copy recombinant strains produced various levels of the target compound DML, illustrating the effectiveness of the iTRDL devices (Figure 3C). In particular, DML synthesis from methanol by the optimum strain A3 was superior to that of our previously constructed P_{AOXI} -based single-copy-producing strain D1 and multicopy-producing strain D9. Moreover, with the predicted optimal combination of expression levels matching pathway genes, we obtained the improved strain Opt (LovB with device intensity of ~450%, LovC and NpgA with device intensity of ~250%, and LovG with device intensity of ~100%). It showed a noticeable advantage over the control strains D1 (5.5-fold for titre and 9.2-fold for productivity) and D9 (2.0-fold for titre and 4.0-fold for productivity). Generally, the DML biosynthetic pathway in Opt was stronger than in the control strains, as reflected by the relative transcription levels of biosynthetic genes (Supplementary Figure S9A). These results verify the strong and flexible expression modes of the engineered iTRDL. Notably, we used only four devices that shared the same DBP–BS pair, whereas 162 iTRDL devices with various DBP–BS pairs provided sufficient optional tools for multigene pathway control. Moreover, we proved the availability of the iTRDL with a statistical experimental design, which can reduce the number of experimental trials, especially for complicated pathways.

With the success of the internal module control by the iTRDL, we next tested the iTRDL- and cTRDL-mediated pathway balancing between the two modules. A full factorial combination of three expression levels from iTRDL (or cTRDL), matching two biosynthetic genes, was designed for the downstream module (Figure 4). These downstream combinations were constructed in the Opt strain, generating nine strains that produced various levels of MJ and intermediates. The optimal expression combination, sLovA, using a device with an intensity of ~250%, and CPR, using a device with an intensity of ~100%, was observed for both the cTRDL and iTRDL. Moreover, the downstream module driven by cTRDL devices achieved an MJ titre which was 20.9% higher than that of iTRDL devices. This finding is in accordance with our previous study (29), which illustrated that constitutive accumulation of downstream enzymes can facilitate conversion of the generated intermediates to the final product after induction. The highest MJ production was obtained from strain OC4 by cTRDL, achieving 3.0- and 1.8-fold titres compared with the control strains J1 and J9, respectively (Figure 4). In addition, the MJ biosynthetic pathway in OC4 and OI4 was stronger than that in the control strains, as reflected by the relative transcription levels of the biosynthetic genes (Supplementary Figure S9B). Generally, it represents the highest reported level of DML and MJ fermented from methanol. Recently, we achieved an MJ production of 3.2 g/l by het-

erologous synthesis of this compound in *P. pastoris* using ethanol as a substrate (29). In addition, a high MJ production of 5.5 g/l from glucose achieved by rewiring metabolic pathways has been reported in the native fungus *Aspergillus terreus* (72). Therefore, there is still room for improvement in the synthesis of MJ using methanol as the sole carbon source. It is worth noting that the DBP–BS pair for devices used in the downstream module was independent of that used in the upstream module. Theoretically, this can avoid the cross-talk of transcriptional regulation control between the two modules. With the effectiveness of the statistically orthogonal experimental design and full factorial design, these synthetic TRDLs may be further applied to complicated pathway regulation using deeper algorithms, such as neural networks and machine learning, in future research. Overall, our TRDLs strengthened and balanced the pathway nodes inside and between the modules. It provides alternative yeast toolboxes for high-level biosynthesis of value-added chemicals from methanol. In addition, these TRDLs should be compatible with heterologous protein expression based on reporter protein levels.

Non-model microorganisms, such as unconventional yeast and filamentous fungi, have been extensively used in many fields, including biopharmaceuticals, novel foods, biorefining, industrial enzymes, platform chemicals, biomaterials and environmental protection. However, these strains are difficult to explore in depth because of their unclear genetic background and insufficient molecular tools. Recently, genetic manipulation tools have become possible using CRISPR–Cas-derived genetic editing technologies. However, accurate expression control systems cannot be easily achieved. Although promoter mining is a common strategy for collecting expression tools, it is difficult to obtain promoters with a high intensity and tight regulation. Ideally, promoters for expression control should be strictly inducible to separate cell growth from protein expression and to avoid a cumulative metabolic burden (51,63). Promoters covering a wide range of intensities are also indispensable for fine-tuning control from tight down-regulation to high overexpression (51). Researchers have modified promoters to breed variants of different strengths. However, the high identity of promoter sequences may cause inter-promoter recombination and transcription titration effects (49–51). Here, we propose a strategy for engineering diverse transcription machinery tools to fine-tune the expression of pathways. This represents a universal construction method of a combinatorial set-up of transactivators, CPs, DBPs and BSs (either native or heterologous), which can be reproduced in extensive methylotrophic hosts.

DATA AVAILABILITY

Details of the construction steps of plasmids and strains and sequences of critical genes are provided in the Supplementary Data. All other data that support the findings of this study are available within the article and the supplementary data, and are also available from the corresponding author upon reasonable request.

SUPPLEMENTARY DATA

[Supplementary Data](#) are available at NAR Online.

FUNDING

This study was supported by the National Key R&D Program of China [2020YFA0907800]; National Natural Science Foundation of China [31870073 and 42176238]; Shanghai Rising-Star Program [19QA1402700]; Shanghai Frontiers Science Center of Optogenetic Techniques for Cell Metabolism [Shanghai Municipal Education Commission]; and Fundamental Research Funds for the Shanghai Science and Technology Innovation Action Plan [17JC1402400]. Funding for open access charge: National Key R&D Program of China [2020YFA0907800]; National Natural Science Foundation of China [31870073 and 42176238].
Conflict of interest statement. None declared.

REFERENCES

- Zhang, Y., Ptacin, J.L., Fischer, E.C., Aerni, H.R., Caffaro, C.E., San Jose, K., Feldman, A.W., Turner, C.R. and Romesberg, F.E. (2017) A semi-synthetic organism that stores and retrieves increased genetic information. *Nature*, **551**, 644–647.
- Robertson, W.E., Funke, L.F.H., de la Torre, D., Fredens, J., Elliott, T.S., Spinck, M., Christova, Y., Cervettini, D., Boge, F.L., Liu, K.C. *et al.* (2021) Sense codon reassignment enables viral resistance and encoded polymer synthesis. *Science*, **372**, 1057–1062.
- Shao, Y., Lu, N., Wu, Z., Cai, C., Wang, S., Zhang, L.L., Zhou, F., Xiao, S., Liu, L., Zeng, X. *et al.* (2018) Creating a functional single-chromosome yeast. *Nature*, **560**, 331–335.
- Luo, J., Sun, X., Cormack, B.P. and Boeke, J.D. (2018) Karyotype engineering by chromosome fusion leads to reproductive isolation in yeast. *Nature*, **560**, 392–396.
- Jiang, W., Hernandez Villamor, D., Peng, H., Chen, J., Liu, L., Haritos, V. and Ledesma-Amaro, R. (2021) Metabolic engineering strategies to enable microbial utilization of C1 feedstocks. *Nat. Chem. Biol.*, **17**, 845–855.
- Conrado, R.J. and Gonzalez, R. (2014) Chemistry. Envisioning the bioconversion of methane to liquid fuels. *Science*, **343**, 621–623.
- Heux, S., Brautaset, T., Vorholt, J.A., Wendisch, V.F. and Portais, J.C. (2018) Synthetic methylotrophy: past, present, and future. In: Kalyuzhnaya, M.G. and Xing, X.-H. (eds). *Methane Biocatalysis: Paving the Way to Sustainability*. Springer International Publishing, Cham, pp. 133–151.
- Meunier, N., Chauvy, R., Mouhoubi, S., Thomas, D. and De Weireld, G. (2020) Alternative production of methanol from industrial CO₂. *Renewable Energy*, **146**, 1192–1203.
- Whitaker, W.B., Sandoval, N.R., Bennett, R.K., Fast, A.G. and Papoutsakis, E.T. (2015) Synthetic methylotrophy: engineering the production of biofuels and chemicals based on the biology of aerobic methanol utilization. *Curr. Opin. Biotechnol.*, **33**, 165–175.
- Meyer, F., Keller, P., Hartl, J., Groninger, O.G., Kiefer, P. and Vorholt, J.A. (2018) Methanol-essential growth of *Escherichia coli*. *Nat. Commun.*, **9**, 1508.
- Whitaker, W.B., Jones, J.A., Bennett, R.K., Gonzalez, J.E., Vernacchio, V.R., Collins, S.M., Palmer, M.A., Schmidt, S., Antoniewicz, M.R., Koffas, M.A. *et al.* (2017) Engineering the biological conversion of methanol to specialty chemicals in *Escherichiacoli*. *Metab. Eng.*, **39**, 49–59.
- Muller, J.E.N., Meyer, F., Litsanov, B., Kiefer, P., Potthoff, E., Heux, S., Quax, W.J., Wendisch, V.F., Brautaset, T., Portais, J.C. *et al.* (2015) Engineering *Escherichiacoli* for methanol conversion. *Metab. Eng.*, **28**, 190–201.
- Lessmeier, L., Pfeifenschneider, J., Carnicer, M., Heux, S., Portais, J.C. and Wendisch, V.F. (2015) Production of carbon-13-labeled cadaverine by engineered *Corynebacterium glutamicum* using carbon-13-labeled methanol as co-substrate. *Appl. Microbiol. Biotechnol.*, **99**, 10163–10176.
- Witthoff, S., Schmitz, K., Niedenführ, S., Nöh, K., Noack, S., Bott, M. and Marienhagen, J. (2015) Metabolic engineering of *Corynebacterium glutamicum* for methanol metabolism. *Appl. Environ. Microbiol.*, **81**, 2215–2225.

15. Tuyishime, P., Wang, Y., Fan, L., Zhang, Q., Li, Q., Zheng, P., Sun, J. and Ma, Y. (2018) Engineering *Corynebacterium glutamicum* for methanol-dependent growth and glutamate production. *Metab. Eng.*, **49**, 220–231.
16. Espinosa, M.I., Williams, T.C., Pretorius, I.S. and Paulsen, I.T. (2019) Benchmarking two *Saccharomyces cerevisiae* laboratory strains for growth and transcriptional response to methanol. *Synth. Syst. Biotechnol.*, **4**, 180–188.
17. Espinosa, M.I., Gonzalez-Garcia, R.A., Valgepea, K., Plan, M.R., Scott, C., Pretorius, I.S., Marcellin, E., Paulsen, I.T. and Williams, T.C. (2020) Adaptive laboratory evolution of native methanol assimilation in *Saccharomyces cerevisiae*. *Nat. Commun.*, **11**, 5564.
18. Dai, Z., Gu, H., Zhang, S., Xin, F., Zhang, W., Dong, W., Ma, J., Jia, H. and Jiang, M. (2017) Metabolic construction strategies for direct methanol utilization in *Saccharomyces cerevisiae*. *Bioresour. Technol.*, **245**, 1407–1412.
19. Zhu, T., Zhao, T., Bankefa, O.E. and Li, Y. (2020) Engineering unnatural methylotrophic cell factories for methanol-based biomanufacturing: challenges and opportunities. *Biotechnol. Adv.*, **39**, 107467.
20. Schwarzjans, J.P., Luttermann, T., Geier, M., Kalinowski, J. and Friehs, K. (2017) Towards systems metabolic engineering in *Pichiapastoris*. *Biotechnol. Adv.*, **35**, 681–710.
21. Yang, Z. and Zhang, Z. (2018) Engineering strategies for enhanced production of protein and bio-products in *Pichiapastoris*: a review. *Biotechnol. Adv.*, **36**, 182–195.
22. Pena, D.A., Gasser, B., Zanghellini, J., Steiger, M.G. and Mattanovich, D. (2018) Metabolic engineering of *Pichiapastoris*. *Metab. Eng.*, **50**, 2–15.
23. Cregg, J.M. and Madden, K.R. (1988) Development of the methylotrophic yeast, *Pichiapastoris*, as a host system for the production of foreign proteins. *Dev. Indust. Microbiol.*, **29**, 33–41.
24. De Schutter, K., Lin, Y.C., Tiels, P., Van Hecke, A., Glinka, S., Weber-Lehmann, J., Rouze, P., Van de Peer, Y. and Callewaert, N. (2009) Genome sequence of the recombinant protein production host *Pichiapastoris*. *Nat. Biotechnol.*, **27**, 561–566.
25. Bill, R.M. (2014) Playing catch-up with *Escherichia coli*: using yeast to increase success rates in recombinant protein production experiments. *Front. Microbiol.*, **5**, 85.
26. Siripong, W., Wolf, P., Kusumoputri, T.P., Downes, J.J., Kocharin, K., Tanapongpipat, S. and Rungphan, W. (2018) Metabolic engineering of *Pichiapastoris* for production of isobutanol and isobutyl acetate. *Biotechnol. Biofuels*, **11**, 1.
27. Yang, Z. and Zhang, Z. (2018) Production of (2R, 3R)-2,3-butanediol using engineered *Pichiapastoris*: strain construction, characterization and fermentation. *Biotechnol. Biofuels*, **11**, 35.
28. Liu, Y., Tu, X., Xu, Q., Bai, C., Kong, C., Liu, Q., Yu, J., Peng, Q., Zhou, X., Zhang, Y. et al. (2018) Engineered monoculture and co-culture of methylotrophic yeast for de novo production of monacolin J and lovastatin from methanol. *Metab. Eng.*, **45**, 189–199.
29. Liu, Y., Bai, C., Liu, Q., Xu, Q., Qian, Z., Peng, Q., Yu, J., Xu, M., Zhou, X., Zhang, Y. et al. (2019) Engineered ethanol-driven biosynthetic system for improving production of acetyl-CoA derived drugs in Crabtree-negative yeast. *Metab. Eng.*, **54**, 275–284.
30. Gassler, T., Sauer, M., Gasser, B., Egermeier, M., Troyer, C., Causon, T., Hann, S., Mattanovich, D. and Steiger, M.G. (2020) The industrial yeast *Pichiapastoris* is converted from a heterotroph into an autotroph capable of growth on CO₂. *Nat. Biotechnol.*, **38**, 210–216.
31. Gassler, T., Baumschabl, M., Sallaberger, J., Egermeier, M. and Mattanovich, D. (2022) Adaptive laboratory evolution and reverse engineering enhances autotrophic growth in *Pichiapastoris*. *Metab. Eng.*, **69**, 112–121.
32. Liu, Q., Shi, X., Song, L., Liu, H., Zhou, X., Wang, Q., Zhang, Y. and Cai, M. (2019) CRISPR-Cas9-mediated genomic multiloci integration in *Pichiapastoris*. *Microb. Cell Fact.*, **18**, 144.
33. Prielhofer, R., Barrero, J.J., Steuer, S., Gassler, T., Zahrl, R., Baumann, K., Sauer, M., Mattanovich, D., Gasser, B. and Marx, H. (2017) GoldenPiCS: a golden Gate-derived modular cloning system for applied synthetic biology in the yeast *Pichiapastoris*. *BMC Syst. Biol.*, **11**, 123.
34. Weninger, A., Hatzl, A.M., Schmid, C., Vogl, T. and Glieder, A. (2016) Combinatorial optimization of CRISPR/Cas9 expression enables precision genome engineering in the methylotrophic yeast *Pichiapastoris*. *J. Biotechnol.*, **235**, 139–149.
35. Weninger, A., Fischer, J.E., Raschmanová, H., Kniely, C., Vogl, T. and Glieder, A. (2018) Expanding the CRISPR/Cas9 toolkit for *Pichiapastoris* with efficient donor integration and alternative resistance markers. *J. Cell. Biochem.*, **119**, 3183–3198.
36. Yang, Y., Liu, G., Chen, X., Liu, M., Zhan, C., Liu, X. and Bai, Z. (2020) High efficiency CRISPR/Cas9 genome editing system with an eliminable episomal sgRNA plasmid in *Pichiapastoris*. *Enzyme Microb. Technol.*, **138**, 109556.
37. Cai, P., Duan, X., Wu, X., Gao, L., Ye, M. and Zhou, Y.J. (2021) Recombination machinery engineering facilitates metabolic engineering of the industrial yeast *Pichiapastoris*. *Nucleic Acids Res.*, **49**, 7791–7805.
38. Gao, J., Xu, J., Zuo, Y., Ye, C., Jiang, L., Feng, L., Huang, L., Xu, Z. and Lian, J. (2022) Synthetic biology toolkit for marker-less integration of multigene pathways into *Pichiapastoris* via CRISPR/Cas9. *ACS Synth. Biol.*, **11**, 623–633.
39. Gao, J., Ye, C., Cheng, J., Jiang, L., Yuan, X. and Lian, J. (2022) Enhancing homologous recombination efficiency in *Pichiapastoris* for multiplex genome integration using short homology arms. *ACS Synth. Biol.*, **11**, 547–553.
40. Nishi, T., Ito, Y., Nakamura, Y., Yamaji, T., Hashiba, N., Tamai, M., Yasohara, Y., Ishii, J. and Kondo, A. (2022) One-step in vivo assembly of multiple DNA fragments and genomic integration in *Komagataella phaffii*. *ACS Synth. Biol.*, **11**, 644–654.
41. Naseri, G., Behrend, J., Rieper, L. and Mueller-Roeber, B. (2019) COMPASS for rapid combinatorial optimization of biochemical pathways based on artificial transcription factors. *Nat. Commun.*, **10**, 2615.
42. Hartner, F.S., Ruth, C., Langenegger, D., Johnson, S.N., Hyka, P., Lin-Cereghino, G.P., Lin-Cereghino, J., Kovar, K., Cregg, J.M. and Glieder, A. (2008) Promoter library designed for fine-tuned gene expression in *Pichiapastoris*. *Nucleic Acids Res.*, **36**, e76.
43. Xuan, Y., Zhou, X., Zhang, W., Zhang, X., Song, Z. and Zhang, Y. (2009) An upstream activation sequence controls the expression of *AOX1* gene in *Pichiapastoris*. *FEMS Yeast Res.*, **9**, 1271–1282.
44. Qin, X., Qian, J., Yao, G., Zhuang, Y., Zhang, S. and Chu, J. (2011) GAP promoter library for fine-tuning of gene expression in *Pichiapastoris*. *Appl. Environ. Microbiol.*, **77**, 3600–3608.
45. Prielhofer, R., Maurer, M., Klein, J., Wenger, J., Kiziak, C., Gasser, B. and Mattanovich, D. (2013) Induction without methanol: novel regulated promoters enable high-level expression in *Pichiapastoris*. *Microb. Cell Fact.*, **12**, 5.
46. Ergün, B.G., Gasser, B., Mattanovich, D. and Çalik, P. (2019) Engineering of alcohol dehydrogenase 2 hybrid-promoter architectures in *Pichiapastoris* to enhance recombinant protein expression on ethanol. *Biotechnol. Bioeng.*, **116**, 2674–2686.
47. Ergün, B.G., Demir, İ., Özdamar, T.H., Gasser, B., Mattanovich, D. and Çalik, P. (2020) Engineered deregulation of expression in yeast with designed hybrid-promoter architectures in coordination with discovered master regulator transcription factor. *Adv. Biosyst.*, **4**, e1900172.
48. Wen, J., Tian, L., Xu, M., Zhou, X., Zhang, Y. and Cai, M. (2020) A synthetic malonyl-CoA metabolic oscillator in *Komagataella phaffii*. *ACS Synth. Biol.*, **9**, 1059–1068.
49. Brewster, R.C., Weinert, F.M., Garcia, H.G., Song, D., Rydenfelt, M. and Phillips, R. (2014) The transcription factor titration effect dictates level of gene expression. *Cell*, **156**, 1312–1323.
50. Huang, M., Gao, Y., Zhou, X., Zhang, Y. and Cai, M. (2017) Regulating unfolded protein response activator HAC1p for production of thermostable raw-starch hydrolyzing α -amylase in *Pichiapastoris*. *Bioprocess Biosyst. Eng.*, **40**, 341–350.
51. Vogl, T., Sturmberger, L., Kickenweiz, T., Wasmayer, R., Schmid, C., Hatzl, A.M., Gerstmann, M.A., Pitzer, J., Wagner, M., Thallinger, G.G. et al. (2016) A toolbox of diverse promoters related to methanol utilization: functionally verified parts for heterologous pathway expression in *Pichiapastoris*. *ACS Synth. Biol.*, **5**, 172–186.
52. Rantasalo, A., Landowski, C.P., Kuivanen, J., Korppoo, A., Reuter, L., Koivistoinen, O., Valkonen, M., Penttilä, M., Jantti, J. and Mojzita, D. (2018) A universal gene expression system for fungi. *Nucleic Acids Res.*, **46**, e111.
53. Zhao, E.M., Zhang, Y., Mehl, J., Park, H., Lalwani, M.A., Toettcher, J.E. and Avalos, J.L. (2018) Optogenetic regulation of engineered cellular metabolism for microbial chemical production. *Nature*, **555**, 683–687.

54. Liu, Q., Song, L., Peng, Q., Zhu, Q., Shi, X., Xu, M., Wang, Q., Zhang, Y. and Cai, M. (2022) A programmable high-expression yeast platform responsive to user-defined signals. *Sci. Adv.*, **8**, eabl5166.
55. Watson, J.D., Baker, T.A., Bell, S.P., Gann, A., Levine, M. and Losick, R. (2014) Transcriptional regulation in eukaryotes. In: Watson, J.D. (ed). *Molecular Biology of the Gene*. 7th edn, Cold Spring Harbor Laboratory Press, NY, Vol. 5, pp.657–666.
56. Wang, X., Chen, X. and Yang, Y. (2012) Spatiotemporal control of gene expression by a light-switchable transgene system. *Nat. Methods*, **9**, 266–269.
57. Wang, X., Wang, Q., Wang, J., Bai, P., Shi, L., Shen, W., Zhou, M., Zhou, X., Zhang, Y. and Cai, M. (2016) Mit1 transcription factor mediates methanol signaling and regulates the *alcohol oxidase 1 (AOX1)* promoter in *Pichiapastoris*. *J. Biol. Chem.*, **291**, 6245–6261.
58. Ottoz, D.S.M., Fabian, R. and Joerg, S. (2014) Inducible, tightly regulated and growth condition-independent transcription factor in *Saccharomyces cerevisiae*. *Nucleic Acids Res.*, **42**, e130.
59. Stanton, B.C., Nielsen, A.A., Tamsir, A., Clancy, K., Peterson, T. and Voigt, C.A. (2014) Genomic mining of prokaryotic repressors for orthogonal logic gates. *Nat. Chem. Biol.*, **10**, 99–105.
60. Lin-Cereghino, G.P., Godfrey, L., de la Cruz, B.J., Johnson, S., Khuongsathiene, S., Tolstorukov, I., Yan, M., Lin-Cereghino, J., Veenhuis, M., Subramani, S. et al. (2006) Mxr1p, a key regulator of the methanol utilization pathway and peroxisomal genes in *Pichiapastoris*. *Mol. Cell. Biol.*, **26**, 883–897.
61. Sahu, U., Krishna Rao, K. and Rangarajan, P.N. (2014) Trm1p, a Zn(II)₂Cys₆-type transcription factor, is essential for the transcriptional activation of genes of methanol utilization pathway, in *Pichiapastoris*. *Biochem. Biophys. Res. Commun.*, **451**, 158–164.
62. Dobi, K.C. and Winston, F. (2007) Analysis of transcriptional activation at a distance in *Saccharomyces cerevisiae*. *Mol. Cell. Biol.*, **27**, 5575–5586.
63. Blazek, J. and Alper, H.S. (2013) Promoter engineering: recent advances in controlling transcription at the most fundamental level. *Biotechnol. J.*, **8**, 46–58.
64. Turkanoglu Ozcelik, A., Yilmaz, S. and Inan, M. (2019) *Pichiapastoris* promoters. *Methods Mol. Biol.*, **1923**, 97–112.
65. Vogl, T., Sturmberger, L., Fauland, P.C., Hyden, P., Fischer, J.E., Schmid, C., Thallinger, G.G., Geier, M. and Glieder, A. (2018) Methanol independent induction in *Pichiapastoris* by simple derepressed overexpression of single transcription factors. *Biotechnol. Bioeng.*, **115**, 1037–1050.
66. Xu, N., Zhu, J., Zhu, Q., Xing, Y., Cai, M., Jiang, T., Zhou, M. and Zhang, Y. (2018) Identification and characterization of novel promoters for recombinant protein production in yeast *Pichiapastoris*. *Yeast*, **35**, 379–385.
67. Liu, Y., Bai, C., Xu, Q., Yu, J., Zhou, X., Zhang, Y. and Cai, M. (2018) Improved methanol-derived lovastatin production through enhancement of the biosynthetic pathway and intracellular lovastatin efflux in methylotrophic yeast. *Bioresour. Bioproc.*, **5**, 22.
68. Wang, Y., Fan, L., Tuyishime, P., Zheng, P. and Sun, J. (2020) Synthetic methylotrophy: a practical solution for methanol-based biomanufacturing. *Trends Biotechnol.*, **38**, 650–666.
69. Zhang, T., Ge, C., Deng, L., Tan, T. and Wang, F. (2015) C4-dicarboxylic acid production by overexpressing the reductive TCA pathway. *FEMS Microbiol. Lett.*, **362**, fnv052.
70. Yamada, R., Ogura, K., Kimoto, Y. and Ogino, H. (2019) Toward the construction of a technology platform for chemicals production from methanol: D-lactic acid production from methanol by an engineered yeast *Pichiapastoris*. *World J. Microbiol. Biotechnol.*, **35**, 37.
71. Cai, P., Wu, X., Deng, J., Gao, L., Shen, Y., Yao, L. and Zhou, Y.J. (2022) Methanol biotransformation toward high-level production of fatty acid derivatives by engineering the industrial yeast *pichiapastoris*. *Proc. Natl Acad. Sci. U.S.A.*, **119**, e2201711119.
72. Huang, X., Tang, S., Zheng, L., Teng, Y., Yang, Y., Zhu, J. and Lu, X. (2019) Construction of an efficient and robust *Aspergillus terreus* cell factory for monacolin J production. *ACS Synth. Biol.*, **8**, 818–825.